Journal of Alloys and Compounds 643 (2015) S283–S286

Contents lists available at ScienceDirect

Journal of Alloys and Compounds

journal homepage: www.elsevier.com/locate/jalcom

Effect of the Heusler phase formation on the magnetic behavior of the Cu–10 wt.%Mn alloy with Al and Ag additions

T.M. Carvalho [a,*], A.T. Adorno [a], C.M.A. Santos [a], R.A.G. Silva [b], M. Magnani [a]

[a] Instituto de Química – UNESP, Caixa Postal 355, 14801-970 Araraquara, SP, Brazil
[b] Departamento de Ciências Exatas e da Terra – UNIFESP, 09972-270 Diadema, SP, Brazil

ARTICLE INFO

Article history:
Available online 19 December 2014

Keywords:
Metals and alloys
Solid state reactions
Precipitation
Microstructure
Magnetic measurements

ABSTRACT

In this work, the formation of the Cu_2AlMn Heusler phase and its influence on the magnetic behavior of the Cu–Mn–Al–Ag alloys in the range of 8–10 wt.% of aluminum and 2–4 wt.% of silver were studied using differential scanning calorimetry (DSC), transmission electron microscopy (TEM), high-resolution TEM (HRTEM) and saturation magnetization measurements at 4 K. The results showed that there is a correlation between the presence of the Ag-rich phase and the formation of the Cu_2MnAl phase.

1. Introduction

Copper-based alloys are widely used in many fields because of their good combination of high thermal and electrical conductivities. In particular, Cu-based alloys with high performance are required in field of electronic materials, such as substrate and lead frame in printed board, interconnection and so on, because the electronic packaging has a tendency to miniaturization [1]. The Cu-Al-Mn alloys are quite interesting, since it can show shape memory effect [2] and magnetic effects [3], depending on the Mn and Al contents.

In Cu-Mn-Al solid solutions, ferromagnetic particles are formed at the early stages of a decomposition process. Aged Cu–Mn–Al alloys undergo a martensitic transformation and have interesting magnetic properties due to their superparamagnetic behavior and giant magnetoresistance. The system of dispersed ferromagnetic inclusions of Cu_2MnAl phase in a non-ferromagnetic matrix Cu_3Al forms as a result of the high-temperature β_1-phase aging [4,5].

Additions in the range of 10–15 wt.% aluminum and 0–10 wt.% of manganese concentrations on the martensitic transformation temperatures and shape memory effect were studied on Cu–Al–Mn alloys and magnetic properties of alloys showed low magnetization [6]. The presence of Ag-rich precipitates can increase the Cu_2MnAl relative fraction, thus promoting modifications in the magnetic properties of the annealed Cu–11 wt.%Al–10 wt.%Mn–3 wt.%Ag alloy [7].

In this work, the formation of the Cu_2AlMn Heusler phase and its influence on the magnetic behavior of the Cu–Mn–Al–Ag alloys in the range of 8–10 wt.% of aluminum and 2–4 wt.% of silver were studied using differential scanning calorimetry (DSC), transmission electron microscopy (TEM), high-resolution TEM (HRTEM) and saturation magnetization measurements at 4 K.

2. Materials and methods

The Cu–10 wt.%Mn–8 wt.%Al–2 wt.%Ag, Cu–10 wt.%Mn–8 wt.%Al–4 wt.%Ag, Cu–10 wt.%Mn–10 wt.%Al–2 wt.%Ag and Cu–10 wt.%Mn–10 wt.%Al–4 wt.%Ag alloys were prepared in an arc furnace under argon atmosphere using 99.95% copper, 99.97% aluminum, 99.99% manganese and 99.98% silver as starting materials. Results from chemical analysis obtained from optical emission spectroscopy indicated a final alloy composition very close to the nominal one, with Pb, Fe, and Mn as main impurities (concentration less than 100 ppm). All samples were annealed during 120 h at 850 °C for homogenization. After homogenization, the samples were initially annealed for 180 min at 850 °C and cooled at a constant rate of 1.0 °C min^{-1}. In sequence the samples were quenched for 1 h at 850 °C and then cooled in ice water. Magnetic measurements were obtained using a vibrating sample magnetometer (PPMS Ever Cool, 9 tesla, Quantum Design). Differential scanning calorimetry (DSC) curves were obtained using a Q20 TA instrument, platinum pan, nitrogen flux at about 50 mL min^{-1} and solid samples with 3.0 mm diameter. After the heat treatments the samples were polished, etched and examined by transmission electron microscopy (TEM) using a JEM 2100 microscope, operating at 200 kV. The TEM micrographs were obtained at the Brazilian Nanotechnology National Laboratory (LNNano). The X-ray diffraction (XRD) patterns were obtained using a Siemens D5000 4B diffractometer, Cu Kα radiation and solid (not powdered) samples.

3. Results and discussion

Fig. 1 shows the plots of magnetic moment changes with applied field obtained at 4 K for the annealed Cu–10 wt.%Mn–8 wt.%

* Corresponding author. Tel.: +55 16 3301 9639; fax: +55 16 3322 2308.
E-mail address: thaisa.mary@gmail.com (T.M. Carvalho).

http://dx.doi.org/10.1016/j.jallcom.2014.12.055
0925-8388/

Al–2 wt.%Ag, Cu–10 wt.%Mn–8 wt.%Al–4 wt.%Ag, Cu–10 wt.%Mn–10 wt.%Al–2 wt.%Ag and Cu–10 wt.%Mn–10 wt.%Al–4 wt.%Ag alloys and for the quenched alloys, respectively. These curves indicate that for the annealed alloys the magnetic saturation value is reached at about 11.80 emu/g for alloys containing 8 wt.%Al and at about 19.30 emu/g for alloys with 10 wt.%Al. For all quenched alloys the magnetic saturation value is reached at about 16.30 emu/g.

Fig. 2a shows the DSC curves obtained with a heating rate of 10 °C min^{-1} for the alloys initially annealed. These curves show two endothermic peaks: the first one, at about 300 °C, is associated with the beginning of decomposition of the T_3-Cu_3Mn_2Al phase. In this same temperature range the $\beta_1(DO_3) + Cu_2AlMn(L2_1)_f \rightarrow Cu_2AlMn(L2_1)_p$ also occurs [4]. The second endothermic peak, at about 500 °C, corresponds to the transitions $Cu_2AlMn(L2_1)_p \rightarrow \beta(B2)$ and $\alpha + T_3\text{-}Cu_3Mn_2Al + \gamma \rightarrow \beta(B2) + T_3\text{-}Cu_3Mn_2Al + \gamma$ [8,9].

Fig. 2b shows the DSC curves obtained with a heating rate of 3 °C min^{-1} for the quenched alloys. These curves show four peaks. The first exothermic peak, at about 300 °C, is associated with α and γ_1 phases precipitation. The second exothermic peak, at about 430 °C, corresponds to the Ag-rich phase precipitation. The third endothermic peak, at about 480 °C, corresponds to the transition $\beta(DO_3) + Cu_2AlMn(L2_1) \rightarrow \beta_1(DO_3)$. The fourth endothermic peak, at about 510 °C corresponds to the Ag-rich phase dissolution and to the $\beta_1(DO_3) \rightarrow \beta_2(B2)$ transition [8]. One additional peak, at about 580 °C, was observed for the Cu–8 wt.%Al–10 wt.% Mn–4 wt.%Ag and Cu–10 wt.%Al–10 wt.%Mn–4 wt.%Ag alloys, which is associated with the transition $\beta_2(B2) \rightarrow \beta(A2)$ [8]. The presence of these phases (Fig. 2a and b) is confirmed by the X-ray diffraction patterns in Fig. 3.

Fig. 4 shows the TEM images obtained for the Cu–8 wt.% Al–10 wt.%Mn–2 wt.%Ag alloy initially annealed and the EDS spectrum obtained on the nanoprecipitates and on the matrix. The size range of these nanoprecipitates is between 11 and 24 nm and corresponds to Ag rich phase with, as shown in Fig. 4b.

Fig. 5 shows the TEM and HRTEM images obtained for the Cu–10 wt.%Al–10 wt.%Mn–4 wt.%Ag alloy initially annealed, where one can observe the presence of nanoprecipitates on the matrix. Experimental data indicate that these precipitates correspond to the Ag-rich phase with zone axis [1 0 1] and mean size at about 15 nm. The Cu_2MnAl phase was detected in the matrix with zone axis [1 1 1]. Fig. 6 shows the TEM images obtained for the quenched alloy, indicating that the Cu_2MnAl and the Ag-rich phases were dissolved in the matrix. This can be related to a decrease in the mean size and an increase of the Cu_2AlMn nanoparticles dispersion.

The results obtained from magnetic measurements seem to confirm what was observed from Figs. 4–6, that there is a

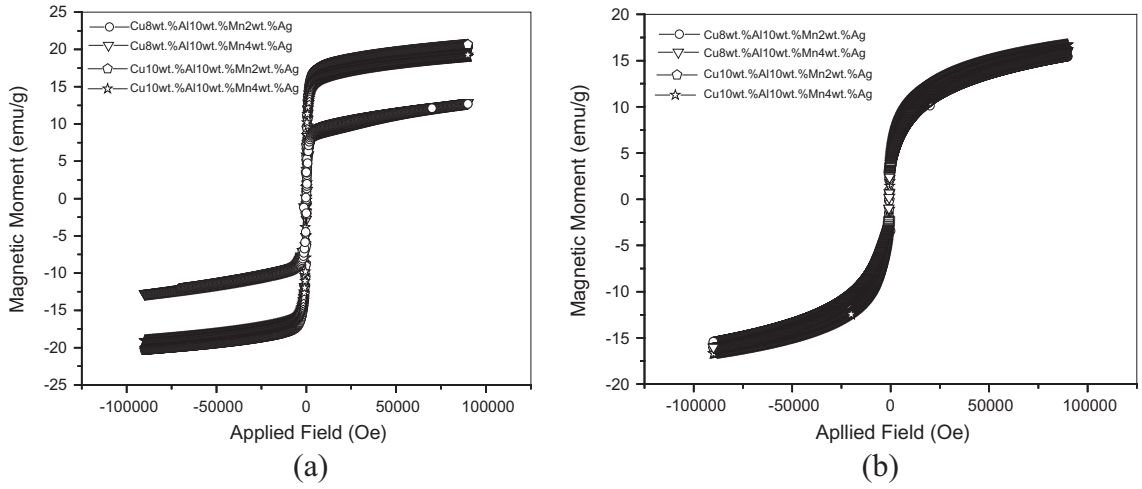

Fig. 1. Magnetic moment change with applied field for the studied alloys (a) initially annealed and (b) quenched from 850 °C in iced water.

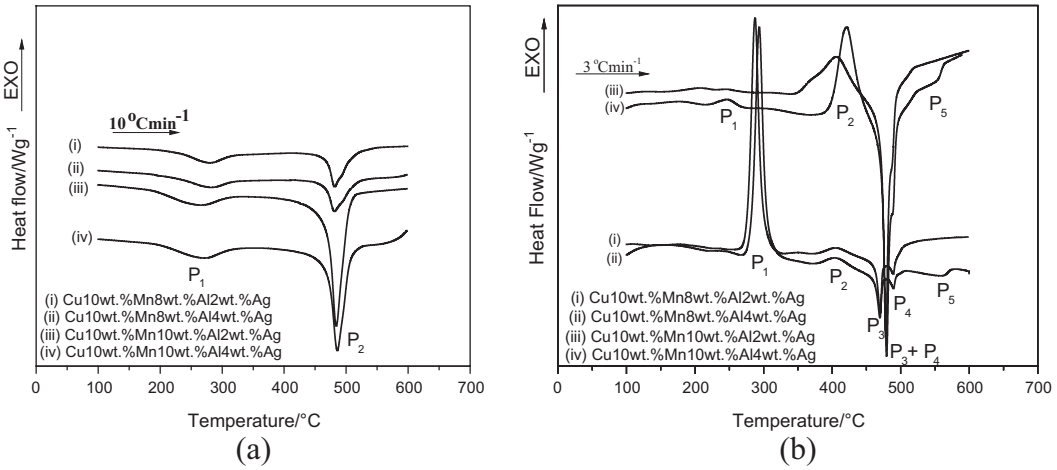

Fig. 2. DSC curves obtained for the studied alloys (a) initially annealed and (b) quenched.

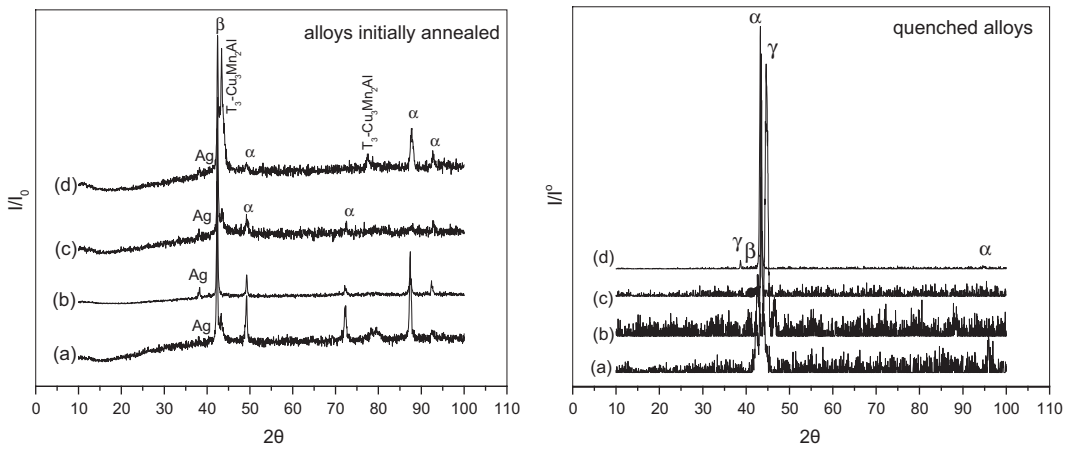

Fig. 3. X-ray diffractions patterns obtained for the (a) Cu–10 wt.%Mn–8 wt.%Al–2 wt.%Ag, (b) Cu–10 wt.%Mn–8 wt.%Al–4 wt.%Ag, (c) Cu–10 wt.%Mn–10 wt.%Al–2 wt.%Ag and (d) Cu–10 wt.%Mn–10 wt.%Al–4 wt.%Ag alloys.

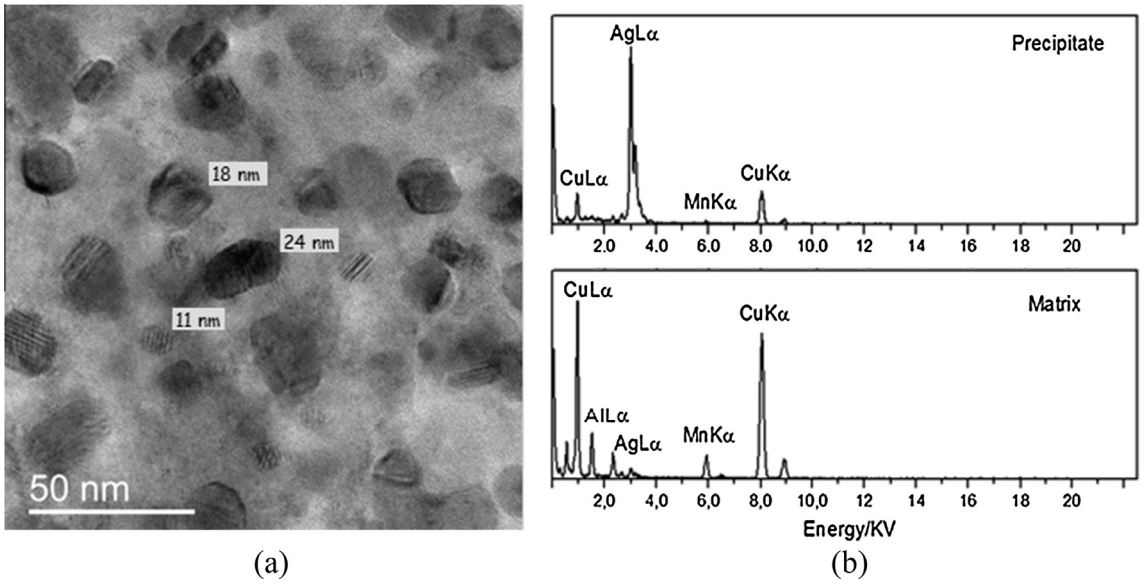

Fig. 4. (a) TEM image obtained for the Cu–8 wt.%Al–10 wt.%Mn–2 wt.%Ag alloy initially annealed and (b) EDS spectra from (a).

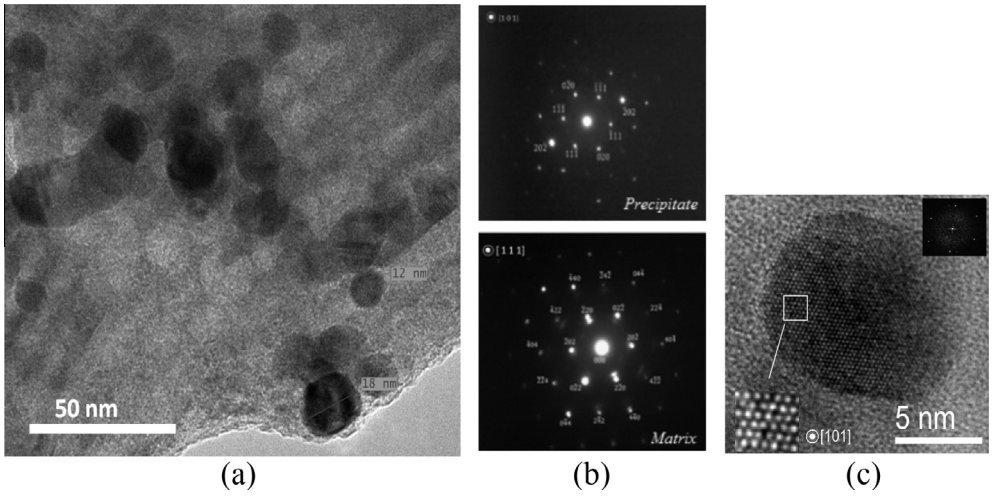

Fig. 5. TEM image obtained for the (a) Cu–10 wt.%Al–10 wt.%Mn–4 wt.%Ag alloys initially annealed; (b) selected-area diffraction pattern (SAED) of the matrix and of the precipitation in (a) and (c) HRTEM image obtained in the Ag-rich phase.

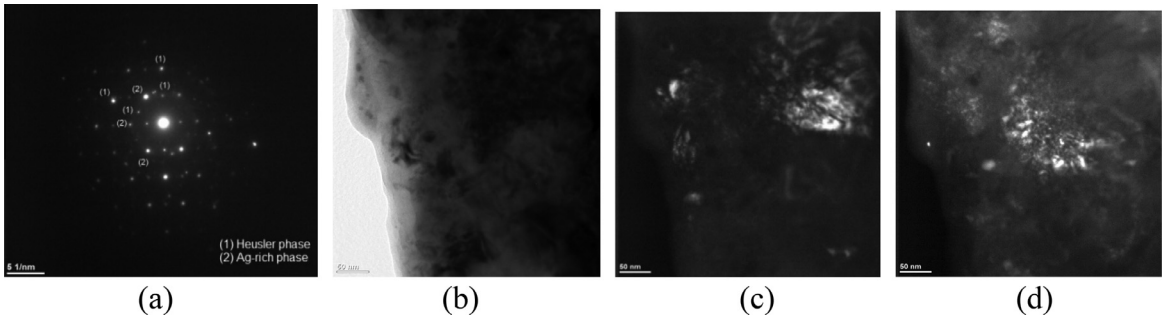

Fig. 6. TEM image obtained for the Cu–10 wt.%Al–10 wt.%Mn–4 wt.%Ag alloy quenched: (a) Selected-area diffraction pattern (SAED); (b) bright-field (BF) electron micrograph of the as-quenched alloy; (c) dark-field (DF) electron micrographs of the Cu_2MnAl phase and (d) DF of the Ag-rich phase.

correlation between the Ag-rich phase and the Cu_2MnAl phase formation. The presence of the Cu_2MnAl phase is observed in quenched alloys but not frequently in annealed alloys, probably because this phase is formed from the quench of the β phase. The alloys studied in this work may be out of the miscibility gap region [10], but Al and Ag additions shift the equilibrium concentration to higher Al values [11] and close to the miscibility gap limit. The occurrence of magnetization and its increase with the increase of Ag concentration, in annealed alloys, seems to confirm that there is a correlation between the presence of the Ag-rich phase and the formation of the Cu_2MnAl phase.

4. Conclusions

The results showed that there is a correlation between the presence of the Ag-rich phase and the formation of the Cu_2MnAl phase. The decrease in the magnetic saturation value is due to changes on the relative fraction of the Cu_2AlMn phase, which is decreased after quenching in the presence of Ag.

Acknowledgements

The authors thank FAPESP (Proc. 2011/19387-7), the Electron Microscopy Laboratory (LME) at Brazilian Nanotechnology National Laboratory (LNNANO) for TEM analysis, Superconducting Materials, electric and magnetic research group the EEL-USP (FAPESP 2009/54001-2) and Quantum Materials research group – GMQ the CCNH-UFABC.

References

[1] H.N. Soliman, N. Habib, Effect of ageing treatment on hardness of Cu–12.5 wt% Al shape memory alloy, Indian J. Phys. 88 (2014) 803–812.
[2] Y. Zheng, C. Li, F. Wan, Y. Long, Cu–Al–Mn alloy with shape memory effect at low temperature, J. Alloys Comp. 441 (2007) 317–322.
[3] L. Yiping, A. Murthy, G.C. Hadjipanayis, H. Wan, Giant magnetoresistance in Cu–Mn–Al, Phys. Rev. B 54 (1996) 3033–3036.
[4] V.V. Kokorin, L.E. Kozlova, A.O. Perekos, On nanoparticles of the ferromagnetic Cu_2MnAl phase in Cu–Al–Mn shape memory alloys, Mater. Sci. Eng. A 481–482 (2008) 542–545.
[5] S. Sugimoto, S. Kondo, H. Nakamura, D. Book, Y. Wang, T. Kagotani, R. Kainuma, K. Ishida, M. Okada, M. Homma, Giant magnetoresistance of Cu Al–Cu MnAl melt-spun ribbons, J. Alloys Comp. 265 (1998) 273–280.
[6] C.A. Canbay, A. Aydogdu, Y. Aydogdu, The investigation of thermal and magnetic properties and microstructure analyses of Cu–Al–Mn shape memory alloys, J. Supercond. Nov. Magn. 24 (2011) 871–877.
[7] R.A.G. Silva, A. Paganotti, S. Gama, A.T. Adorno, T.M. Carvalho, C.M.A. Santos, Investigation of thermal, mechanical and magnetic behaviors of the Cu–11%Al alloy with Ag and Mn additions, Mater. Charact. 75 (2013) 194–199.
[8] E. Obradó, C. Frontera, L. Manosa, A. Planes, Order-disorder transitions of Cu–Al–Mn shape memory alloys, Phys. Rev. B: Condens. Matter Mater. 58 (1) (1998) 14245–14255.
[9] A.T. Adorno, M.R. Guerreiro, R.A.G. Silva, Aging kinetics in the Cu–8 wt.%Al alloy with Ag additions, J. Alloys Comp. 354 (2003) 165–170.
[10] M. Bouchard, G. Thomas, Phase transitions and modulated strucutes in ordered $(Cu–Mn)_3Al$, Acta Metall. 23 (1975) 1485–1500.
[11] R.A.G. Silva, A. Cuniberti, M. Stipcich, A.T. Adorno, Effect of Ag addition on the martensitic phase of the Cu–10 wt.% Al alloy, Mater. Sci. Eng. A 456 (2007) 5–10.